

Synthesis and characterization of the open-framework magnesium aluminophosphate UiO-28

Kjell Ove Kongshaug, Helmer Fjellvåg* and Karl Petter Lillerud

Department of Chemistry, University of Oslo, P. O. Box 1033 Blindern, N-0315 Oslo, Norway.
E-mail: helmer.fjellvag@kjemi.uio.no

Received 30th October 2000, Accepted 30th January 2001
First published as an Advance Article on the web 6th March 2001

The synthesis and crystal structures of a new magnesium aluminophosphate and its high temperature variant are described. The as-synthesized material (UiO-28-as), of composition $\text{MgAl}_3(\text{PO}_4)_4 \cdot \text{C}_4\text{N}_3\text{H}_{14} \cdot \text{H}_2\text{O}$, crystallizes in the orthorhombic space group *Pbcm* (no. 57) with $a=9.2769(8)$, $b=14.798(1)$, $c=14.611(1)$ Å and $V=2005.8(3)$ Å³. UiO-28-as has a two-dimensional eight-ring channel system, and is isostructural with a cobalt aluminophosphate (ACP-2) and a cobalt gallophosphate (GCP-2). Aluminium and magnesium are not uniformly distributed over the three non-equivalent metal framework sites. One site contains solely aluminium; one is Al-rich and the third is Mg-rich, leading to an overall Al/Mg ratio of 3. The magnesium-rich metal atom site is partly coordinated by five water molecules. These water molecules can be removed, leading to an anhydrous variant at 175 °C (UiO-28-175). UiO-28-175, of composition $\text{MgAl}_3(\text{PO}_4)_4 \cdot \text{C}_4\text{N}_3\text{H}_{14}$, crystallizes in the orthorhombic space group *Pbcm* (no. 57) with $a=9.2186(4)$, $b=14.8652(4)$, $c=14.5811(4)$ Å and $V=1998.1(2)$ Å³. This material represents a new tetrahedral zeolite topology. The framework is built from an octameric secondary building unit (SBU) which, by vertex sharing, forms layers that are stacked along [100]. The layers are connected by means of covalent P–O–M bonds into a 3D framework. The same octameric SBUs have been identified in the ZON and AFR topologies, and in the gallium phosphate TMP-GaPO.

Introduction

Substitutional solid solution in dense oxides concerns the replacement of an element in the crystalline framework by another element with similar cation radius and coordination. This concept also applies to open-framework aluminophosphates, and such substitutions are important since they may give rise to new materials with interesting properties. Currently, 17 elements are reported to replace Al^{3+} and/or P^{5+} in AlPO_4 materials.¹ In the case of heterovalent substituents in ionic or semiconducting materials, a mechanism for charge balancing is required. In dense oxides, this is typically achieved by defect formation (vacancies or interstitials) or redox processes. In the case of lower valent substituents in open framework structures, charge balance is normally achieved by introduction of (acidic) protons, or, alternatively, by positively charged organic templates.

The highest degree of heterovalent substitution for Al^{3+} by a divalent element was, until recently, 38% in $\text{CoAlPO}_4 \cdot 50\text{H}_2\text{O}$.² However, Stucky and coworkers have now prepared open-framework aluminophosphates with larger amounts of divalent elements incorporated in the structures.^{3,4} Many of these structures are related to the aluminosilicate zeolites with frameworks composed of vertex-sharing tetrahedra. Among the structures, there are both analogs of known structure types, and novel structure types. One of the new structures is ACP-2,³ a 3D open-framework cobalt aluminophosphate (molar ratio Co/Al=3; also existing as a cobalt gallophosphate GCP-2). The present paper reports on the synthesis and crystal structure of a magnesium aluminophosphate denoted UiO-28, which is isostructural with ACP-2. The thermal behaviour of the material was investigated, and a high temperature variant appears at 175 °C (UiO-28-175). This material represents a new fully tetrahedral zeolite topology built from an octameric secondary building unit (SBU). Special emphasis is put on describing the new topology in terms of this SBU, and to relate it to other topologies built from the same SBU.

Experimental

Synthesis

UiO-28 was prepared by mixing $\text{Mg}_3(\text{PO}_4)_2 \cdot 8\text{H}_2\text{O}$ (Fluka), pseudoboehmite (75.6% Al_2O_3), H_3PO_4 (85%), diethylenetriamine ($\text{C}_4\text{N}_3\text{H}_{13}$, 99%, Aldrich) and H_2O in a molar ratio of 0.33 : 0.5 : 2 : 1.5 : 50. The mixture, with an initial pH of 6.4, was heated at 180 °C for 1 day in a teflon-lined steel autoclave. The final pH after the crystallization was 8.4. The product was recovered by filtration, washed with water and dried in air at 60 °C.

Single crystal analysis

A suitable single crystal was mounted on a thin glass fibre and intensity data covering a hemisphere of reciprocal space was collected at 150 K with a Siemens Smart CCD diffractometer ($\Delta\theta=0.3^\circ$; 30 s per frame). Data reduction was performed with the SAINT software,⁵ and empirical absorption correction was carried out using the program SADABS.⁶ The structure was solved and refined using the SHELXTL program package.⁷

The crystal structure of UiO-28-as, $\text{MgAl}_3(\text{PO}_4)_4 \cdot \text{C}_4\text{N}_3\text{H}_{14} \cdot \text{H}_2\text{O}$, was solved in the orthorhombic space group *Pbcm* (no. 57). The direct method solution located all the framework positions. Difference Fourier maps located the template C and N positions. The secondary nitrogen in diethylenetriamine (N2) is disordered over two positions, and was refined with constant occupancy of 0.5. There are three crystallographically distinct metal atom framework sites. On the basis of bond distance considerations, the occupancy for Mg and Al for these sites was fixed (0.82 Al and 0.18 Mg for M1, 1.0 Al for M2 and 0.3 Al and 0.7 Mg for M3). Further difference Fourier maps revealed two residual peaks about 2.3 and 3.8 Å from the M3 site (interpeak distance about 1.5 Å). These peaks were interpreted as two water sites, and the sum of their occupancies was fixed to unity. No hydrogen positions could be located from the data. The last cycles of the least

Table 1 Crystal and structure refinement data for UiO-28-as

Empirical formula	MgAl ₃ (PO ₄) ₄ C ₄ N ₃ H ₁₄ H ₂ O
Formula weight	607.33
Temperature	150 K
Crystal system	Orthorhombic
Space group	<i>Pbcm</i> (no. 57)
Unit cell dimensions	<i>a</i> = 9.2769(8) Å <i>b</i> = 14.798(1) Å <i>c</i> = 14.611(1) Å
Volume	2005.8(3) Å ³
Z	4
Reflections collected	13700
Independent reflections	1370 [<i>R</i> (int) = 0.1182]
Final <i>R</i> indices [<i>I</i> > 2σ(<i>I</i>)]	<i>R</i> ₁ = 0.0923, <i>wR</i> ₂ = 0.2536
<i>R</i> indices (all data)	<i>R</i> ₁ = 0.1078, <i>wR</i> ₂ = 0.2836

squares refinement included atomic positions and anisotropic displacement parameters for all atoms. Unit cell data and relevant parameters for the data collection and the refinement are given in Table 1. The refinement ended in rather high residual factors (Table 1). Attempts to refine the structure in the non-centrosymmetric space group *Pca*2₁ did not improve matters. The high residual factors are probably due to poor crystal quality. The final atomic coordinates and equivalent isotropic displacement parameters are given in Table 2, with selected bond distances and angles in Table 3.

CCDC reference number 1145/274. See <http://www.rsc.org/suppdata/jm/b0/b008728i/> for crystallographic files in .cif format.

Thermogravimetric analysis (TGA)

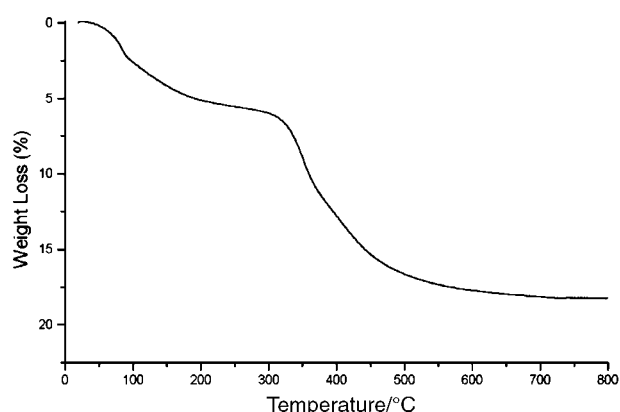
TGA data were obtained on a Scientific Rheometric STA 1500. The sample was heated to 800 °C in a flow of nitrogen gas at a heating rate of 5 K min⁻¹. The TGA curve (Fig. 1) shows two distinct weight losses. The first weight loss of 7% up to around 200 °C is larger than the theoretical 3% loss corresponding to the water molecule in MgAl₃(PO₄)₄·C₄N₃H₁₄·H₂O. This discrepancy is considered to indicate the presence of amorphous impurity phases in the synthesis batch, however, it could also be caused by weakly absorbed water leaving the material below 100 °C. The second, broad weight loss is caused by the organic diethylenetriamine leaving the material.

Table 2 Atomic coordinates and equivalent isotropic displacement parameters (Å²) for UiO-28-as

Atom	<i>x</i>	<i>y</i>	<i>z</i>	<i>U</i> (eq)	Occupancy
P1	0.8765(3)	0.3430(2)	0.2500	0.046(1)	
P2	0.6820(3)	-0.0279(2)	0.2500	0.041(1)	
P3	0.1482(3)	0.1334(2)	0.1031(2)	0.050(1)	
Al1	0.1426(3)	0.3470(2)	0.1150(2)	0.048(1)	0.82
Mg1	0.1426(3)	0.3470(2)	0.1150(2)	0.048(1)	0.18
Al2	0.9015(4)	0.1356(2)	0.2500	0.045(1)	
Al3	0.3323(4)	0.0204(2)	0.2500	0.042(1)	0.30
Mg3	0.3323(4)	0.0204(2)	0.2500	0.042(1)	0.70
O1	0.8256(10)	0.2444(5)	0.2500	0.059(2)	
O2	0.7471(11)	0.4018(6)	0.2500	0.075(3)	
O3	0.9667(8)	0.3592(4)	0.1638(5)	0.071(2)	
O4	0.7559(13)	0.0616(7)	0.2500	0.093(4)	
O5	0.5265(11)	-0.0138(8)	0.2500	0.098(4)	
O6	0.7279(9)	-0.0783(6)	0.3337(6)	0.095(3)	
O7	0.2562(9)	0.0668(5)	0.1397(5)	0.086(3)	
O8	0.1270(10)	0.1149(5)	0.0007(4)	0.078(2)	
O9	0.0026(8)	0.1206(4)	0.1490(5)	0.072(2)	
O10	0.1983(7)	0.2308(4)	0.1167(5)	0.063(2)	
OW1	0.4385(35)	0.1583(18)	0.2500	0.14(2)	0.48
OW2	0.5019(46)	0.2552(38)	0.2500	0.35(5)	0.52
N1	0.2130(12)	-0.0840(8)	0.0054(7)	0.087(3)	
N2	0.6248(26)	0.2425(14)	0.0481(17)	0.099(7)	0.5
C1	0.3689(18)	-0.0966(13)	-0.0138(13)	0.136(7)	
C2	0.4356(19)	-0.1743(12)	0.4729(14)	0.131(6)	

Table 3 Bond lengths (Å) and angles (°) for UiO-28-as

P1–O2	1.482(9)	O2–P1–O3	110.6(4)
P1–O3	1.531(7)	O2–P1–O3	110.6(4)
P1–O3	1.531(7)	O3–P1–O3	110.7(6)
P1–O1	1.534(8)	O2–P1–O1	108.0(6)
		O3–P1–O1	108.5(3)
		O3–P1–O1	108.5(3)
P2–O5	1.458(11)	O5–P2–O4	109.1(7)
P2–O4	1.491(11)	O5–P2–O6	110.7(4)
P2–O6	1.494(7)	O4–P2–O6	108.2(5)
P2–O6	1.494(8)	O5–P2–O6	110.7(4)
		O4–P2–O6	108.2(5)
		O6–P2–O6	109.9(7)
P3–O7	1.504(7)	O7–P3–O9	110.7(4)
P3–O9	1.520(7)	O7–P3–O10	111.7(5)
P3–O10	1.526(7)	O9–P3–O10	109.3(4)
P3–O8	1.534(6)	O7–P3–O8	108.4(5)
		O9–P3–O8	107.1(5)
		O10–P3–O8	109.6(4)
Al1–O8	1.788(6)	O8–Al1–O3	105.7(4)
Al1–O3	1.789(7)	O8–Al1–O6	104.7(4)
Al1–O6	1.796(8)	O3–Al1–O6	112.5(4)
Al1–O10	1.797(7)	O8–Al1–O10	109.8(3)
		O3–Al1–O10	110.7(3)
		O6–Al1–O10	113.0(4)
Al2–O4	1.739(10)	O4–Al2–O1	105.4(5)
Al2–O1	1.758(8)	O4–Al2–O9	109.5(3)
Al2–O9	1.763(7)	O1–Al2–O9	109.1(3)
Al2–O9	1.763(7)	O4–Al2–O9	109.5(3)
		O1–Al2–O9	109.1(3)
		O9–Al2–O9	113.7(5)
Mg3–O5	1.871(11)	O5–Mg3–O7	117.3(3)
Mg3–O7	1.888(7)	O5–Mg3–O7	117.3(3)
Mg3–O7	1.888(7)	O7–Mg3–O7	117.1(5)
Mg3–O2	1.904(9)	O5–Mg3–O2	97.1(5)
Mg3–OW1	2.27(3)	O7–Mg3–O2	101.0(3)
		O7–Mg3–O2	101.0(3)
		O5–Mg3–OW1	79.9(9)
		O7–Mg3–OW1	80.5(5)
		O7–Mg3–OW1	80.5(5)
		O2–Mg3–OW1	177.0(9)
OW1–OW2	1.55(6)	C2–N2–N2	69.1(17)
N1–C1	1.48(2)	C2–N2–C2	105.5(19)
N2–C2	1.39(3)	N2–N2–C2	54.4(14)
N2–N2	1.42(5)	C2–C1–N1	116.2(14)
N2–C2	1.59(3)	N2–C2–C1	128.9(19)
C1–C2	1.44(2)	N2–C2–N2	56.5(19)
		C1–C2–N2	93.9(17)

**Fig. 1** TGA data for UiO-28 on heating to 800 °C in nitrogen at a rate of 5 K min⁻¹.

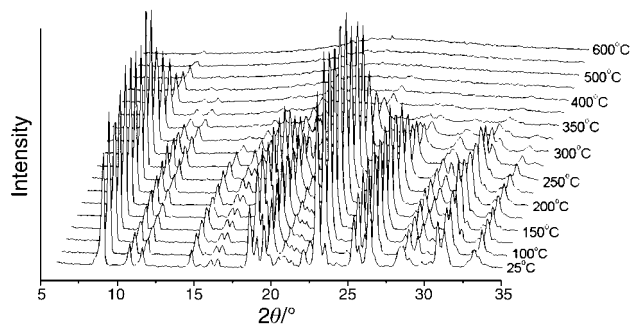


Fig. 2 3D representation of high temperature powder X-ray data for UiO-28 between 25 and 600 °C.

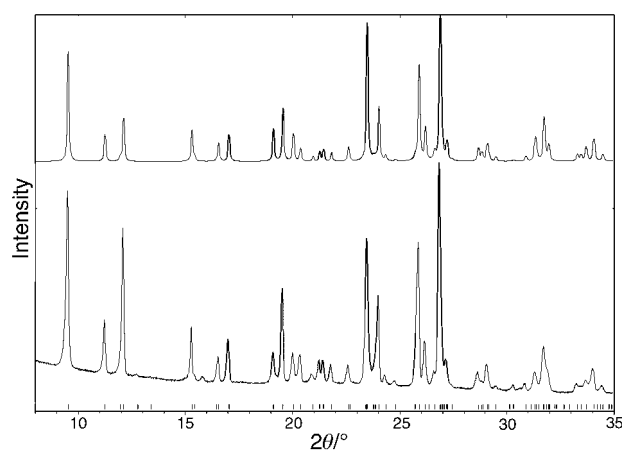


Fig. 3 Simulated (top) and experimental (bottom) powder X-ray diffraction patterns of UiO-28-as.

High temperature powder X-ray diffraction (HT-PXRD)

HT-PXRD data were collected using a Bühler furnace on a Siemens D500 instrument in Bragg–Brentano geometry with Cu-K α radiation. The sample was smeared on a platinum filament and data were collected at 25 °C, between 100 and 400 °C in steps of $\Delta T=25$ °C, and between 400 and 600 °C in steps of $\Delta T=50$ °C. The three dimensional representation of the high temperature powder diffraction patterns (Fig. 2) indicates that UiO-28 remains stable during the first weight loss when the water molecule leaves the material. The anhydrous phase emerges fully at 175 °C (UiO-28-175). There is a reversible dehydration–rehydration process between UiO-28-as and UiO-28-175. The loss of the organic species results in

Table 4 Experimental conditions and relevant data for Rietveld refinements of UiO-28-175

Empirical formula	MgAl ₃ (PO ₄) ₄ C ₄ N ₃ H ₁₄
Formula weight	597.96
Pattern range 2θ	8–90°
Step size $\Delta 2\theta$	0.015576° ^a
Wavelength	1.540598 Å
Space group	<i>Pbcm</i> (no. 57)
Unit cell dimensions	$a=9.2186(4)$ Å $b=14.8652(4)$ Å $c=14.5811(4)$ Å
Volume	1998.1(2) Å ³
Z	4
No. observations	5257
No. reflections	883
No. refined parameters	90
R_{wp}	0.0624
R_{F^2}	0.0790

^aDefined by the PSD setting.

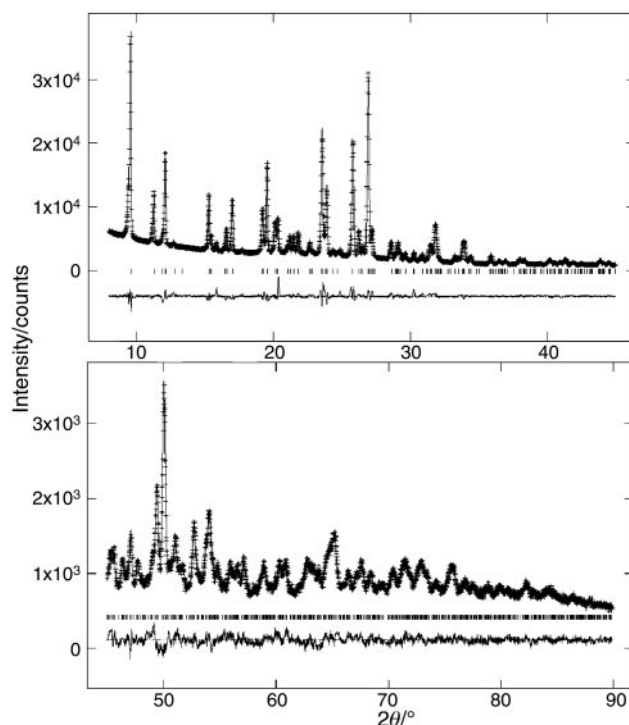


Fig. 4 Observed, calculated and difference powder X-ray diffraction profiles for UiO-28-175.

UiO-28-175 being transformed into an amorphous phase (Fig. 2).

Powder X-ray diffraction

UiO-28-175 was obtained by calcination at 175 °C in air. High resolution powder X-ray diffraction data for this sample and for a sample of UiO-28-as was collected in 0.5 mm sealed capillaries at 25 °C. The experiments were performed with a Siemens D5000 diffractometer with monochromatic Cu-K α ₁ radiation selected with an incident beam germanium monochromator. The detector was a Braun PSD. The diffraction patterns were collected over the 2θ range 8–90°. Total counting time was around 24 h. Fig. 3 reveals a close correspondence between the experimental powder pattern of UiO-28-as and

Table 5 Atomic coordinates and equivalent isotropic displacement parameters (Å²) for UiO-28-175

Atom	<i>x</i>	<i>y</i>	<i>z</i>	<i>U</i> (eq)	Occupancy
P1	0.8890(14)	0.3347(7)	0.2500	0.030(2)	
P2	0.6851(15)	−0.0362(7)	0.2500	0.030(2)	
P3	0.1548(9)	0.1356(5)	0.1041(6)	0.030(2)	
Al1	0.1480(10)	0.3479(5)	0.1145(7)	0.040(2)	0.82
Mg1	0.1480(10)	0.3479(5)	0.1145(7)	0.040(2)	0.18
Al2	0.8989(15)	0.1353(8)	0.2500	0.040(2)	
Mg3	0.3291(19)	0.0190(8)	0.2500	0.040(2)	0.70
Al3	0.3291(19)	0.0190(8)	0.2500	0.040(2)	0.30
O1	0.8144(16)	0.2430(10)	0.2500	0.055(2)	
O2	0.7572(19)	0.3946(12)	0.2500	0.055(2)	
O3	0.9725(13)	0.3597(8)	0.1628(8)	0.055(2)	
O4	0.7563(21)	0.0537(10)	0.2500	0.055(2)	
O5	0.5315(18)	−0.0061(17)	0.2500	0.055(2)	
O6	0.7280(15)	−0.0737(8)	0.3398(7)	0.055(2)	
O7	0.2674(16)	0.0695(8)	0.1364(9)	0.055(2)	
O8	0.1269(13)	0.1116(6)	0.0026(8)	0.055(2)	
O9	0.0134(13)	0.1191(8)	0.1526(9)	0.055(2)	
O10	0.2102(11)	0.2328(7)	0.1187(7)	0.055(2)	
N1	0.2174(14)	−0.0856(9)	−0.0038(18)	0.080(4)	
N2	0.6458(26)	0.2208(16)	0.0528(19)	0.080(4)	0.5
C1	0.3775(16)	−0.1031(10)	−0.0106(25)	0.080(4)	
C2	0.4177(18)	−0.1908(12)	0.4627(17)	0.080(4)	

Table 6 Bond lengths (Å) and angles (°) for UiO-28-175

P1–O1	1.528(10)	O1–P1–O2	99.5(12)
P1–O2	1.506(11)	O1–P1–O3	116.2(8)
P1–O3	1.532(7)	O1–P1–O3	116.2(8)
P1–O3	1.532(7)	O2–P1–O3	105.2(9)
		O2–P1–O3	105.2(9)
		O3–P1–O3	112.2(14)
P2–O4	1.490(10)	O4–P2–O5	98.6(14)
P2–O5	1.485(11)	O4–P2–O6	102.7(9)
P2–O6	1.477(7)	O4–P2–O6	102.7(9)
P2–O6	1.477(7)	O5–P2–O6	111.7(9)
		O5–P2–O6	111.7(9)
		O6–P2–O6	124.9(14)
P3–O7	1.504(9)	O7–P3–O8	105.3(9)
P3–O8	1.545(9)	O7–P3–O9	110.2(10)
P3–O9	1.503(9)	O7–P3–O10	109.9(9)
P3–O10	1.547(9)	O8–P3–O9	105.6(9)
		O8–P3–O10	113.7(7)
		O9–P3–O10	112.0(8)
Al1–O3	1.773(9)	O3–Al1–O6	112.1(8)
Al1–O6	1.764(9)	O3–Al1–O8	104.0(8)
Al1–O8	1.820(9)	O3–Al1–O10	111.7(7)
Al1–O10	1.806(8)	O6–Al1–O8	101.8(7)
		O6–Al1–O10	114.0(9)
		O8–Al1–O10	112.3(6)
Al2–O1	1.780(10)	O1–Al2–O4	106.7(11)
Al2–O4	1.788(10)	O1–Al2–O9	112.3(7)
Al2–O9	1.786(7)	O1–Al2–O9	112.3(7)
Al2–O9	1.786(7)	O4–Al2–O9	110.1(8)
		O4–Al2–O9	110.1(8)
		O9–Al2–O9	105.4(13)
Mg3–O2	2.014(15)	O2–Mg3–O5	102.0(11)
Mg3–O5	1.903(15)	O2–Mg3–O7	104.1(8)
Mg3–O7	1.905(10)	O2–Mg3–O7	104.1(8)
Mg3–O7	1.905(10)	O5–Mg3–O7	111.7(8)
		O5–Mg3–O7	111.7(8)
		O7–Mg3–O7	120.8(12)
N1–C1	1.502(11)	C2–N2–C2	88.6(22)
N2–N2	1.77(6)	N1–C1–C2	110.8(16)
N2–C1	1.868(29)	N2–C2–C1	76.1(15)
N2–C2	1.506(11)	N2–C2–C1	138.1(22)
N2–C2	1.456(12)		

that simulated on the basis of the single crystal determination. This proves that the crystallite chosen for the single crystal analysis of UiO-28-as was representative for the bulk sample. The impurity phase(s) indicated by TGA must therefore be amorphous.

The diffraction pattern of UiO-28-175 was indexed from the first 20 Bragg reflections with the program TREOR-90⁸ leading to an orthorhombic unit cell: $a=9.295$, $b=14.828$ and $c=14.642$ Å ($M_{20}=19$). A careful inspection of the powder pattern indicated space group $Pbcm$ (no. 57); *i.e.* the same space group as for UiO-28-as. Also the unit cell parameters are clearly related (Tables 1 and 4). Hence a starting model for the structure of UiO-28-175 could be built based on the structure of UiO-28-as. This starting model was transferred into the GSAS program⁹ for Rietveld refinements. The occupations of Mg and Al on the metal atom framework sites were fixed to those determined for UiO-28-as. Initially, scale, background, zero point and unit cell parameters were refined. Atomic positions were refined after introduction of soft constraints: $d(\text{P–O})=1.53(2)$, $d(\text{M1–O})=1.79(2)$, $d(\text{Al2–O})=1.75(2)$, $d(\text{M3–O})=1.89(2)$, $d(\text{N–C})=1.48(2)$ and $d(\text{C–C})=1.52(2)$ Å. Common isotropic displacement parameters were adopted for P, the metal atoms and the template C and N. The refinement converged to satisfactory residual factors $R_{F2}=0.0624$ and $R_{wp}=0.0790$. The weight on the soft constraints could not, however, be completely relaxed without unrealistic bond

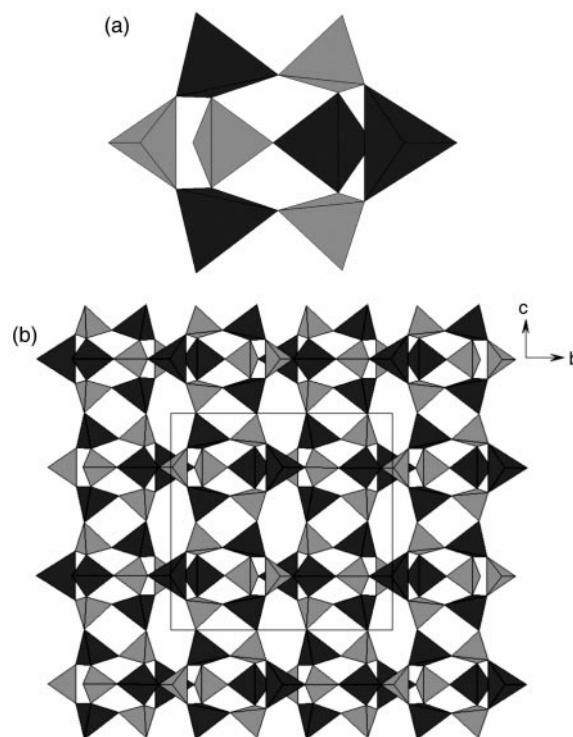


Fig. 5 (a) Polyhedral representation of the octameric building unit in UiO-28, and (b) the arrangement obtained by vertex sharing of octameric units into 2D layers stacked along [100]. MO₄ tetrahedra with darker shading, PO₄ tetrahedra with lighter shading.

distances emerging in the structure. Details of the refinement are given in Table 4. A final Rietveld plot for the refinement is shown in Fig. 4. Atomic coordinates and isotropic displacement parameters and selected bond distances and angles are given in Tables 5 and 6.

Results and discussion

There are three crystallographically distinct metal atom sites in UiO-28-as. Of these, M1 takes a general 8-fold position, while M2 and M3 take special 4-fold positions. The average M–O bond distances are $d(\text{M1–O})=1.792$, $d(\text{M2–O})=1.757$ and $d(\text{M3–O})=1.887$ Å. Since the Mg–O and Al–O bond distances differ significantly, 1.949 *versus* 1.757 Å for CN=4, as derived from bond valence parameters,¹⁰ these bond distances indicate an uneven distribution of Al and Mg at the different sites. An indirect way to evaluate the Mg/Al ratio of UiO-28-as, and also for each site, is through the metal–oxygen bond distances. The M2 site is obviously a pure Al site, whereas M1 is Al-rich. M3 is an Mg-rich site, and it is not surprising that just this site is partly coordinated by additional water, since Mg has a strong affinity towards increased coordination. If one assumes the simple relationship between bond distance and occupancy factor of magnesium: $d(\text{M–O})=1.757+0.192 \times \text{occupancy of magnesium}$, the Mg occupancies are 0.18, 0.00 and 0.70 for M1, M2 and M3, respectively. The average M–O distance in UiO-28-as is 1.807 Å, and this suggests an overall Al/Mg ratio of 3. This is different from the ACP-2 structure where the Co/Al ratio is 3.³ In both cases, the negative charge on the framework is compensated for by protonation of the organic template.

The 3D open-framework structure of UiO-28-as is built from vertex-sharing tetrahedra. However, UiO-28-as, like ACP-2 and GCP-2, cannot be described as exhibiting a four-connected tetrahedral zeolite-like framework, since one site (M3) tends to be five-coordinate. The fifth oxygen stems from a water molecule that has two statistical locations (separated by

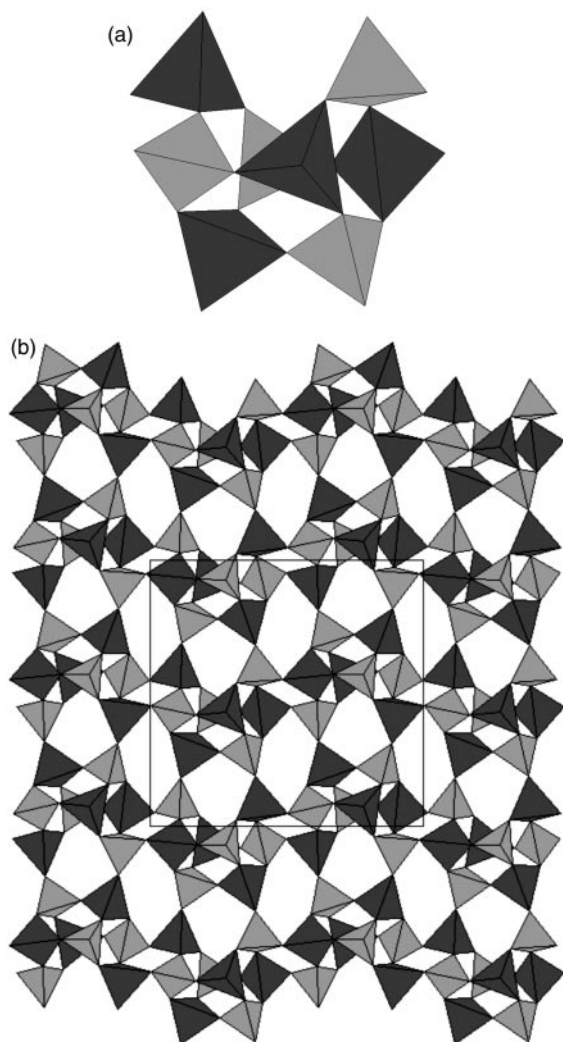


Fig. 6 (a) Polyhedral representation of the octameric building unit in ZON, and (b) the arrangement obtained by vertex sharing of octameric units into 2D layers. AlO_4 tetrahedra with darker shading, PO_4 tetrahedra with lighter shading.

1.55 Å). The M3–OW1 distance is 2.27 Å. Similar non-tetrahedral coordination is also known for UCSB-5.¹¹

UiO-28 possesses a two-dimensional 8-ring channel system along [010] and [001] with dimensions of 6.4×7.3 and 6.1×7.4 Å, respectively. The channels encapsulate diethylenetriamine, which must be monoprotonated in order to compensate for the negative charge on the framework. There are several rather long hydrogen bonding interactions between the amine and the framework [$d(\text{N1} \cdots \text{O3}) = 2.97$, $d(\text{N1} \cdots \text{O7}) = 3.00$, $d(\text{N1} \cdots \text{O8}) = 3.05$ and $d(\text{N1} \cdots \text{O9}) = 3.06$ Å]. The secondary nitrogen (N2) is disordered over two positions, and forms no hydrogen bonding interactions with the framework.

The water molecule in UiO-28-as can be removed by heating without causing collapse of the structure, *cf.* thermal data in Figs. 1 and 2. The dehydrated form, UiO-28-175, represents a new fully tetrahedral zeolite topology. The framework is built from an octameric secondary building unit (Fig. 5a), which is formed from four PO_4 and four MO_4 tetrahedra. The framework can be described as layers stacked in the [100] direction. These layers are composed of vertex-sharing building units involving four different orientations (Fig. 5b). The layers are connected *via* P–O–M bonds and a two-dimensional 8-ring channel system exists. The octameric SBU present in UiO-28 has earlier been identified in the ZON^{12–14} and AFR^{15–17} topologies (depicted in different perspectives in Figs. 6a and

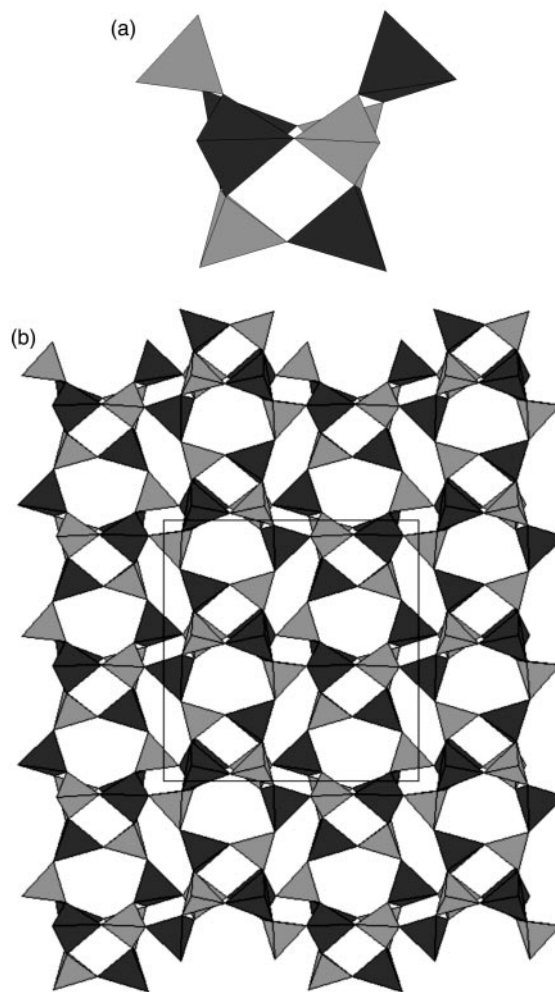


Fig. 7 (a) Polyhedral representation of the octameric building unit in AFR, and (b) the arrangement obtained by vertex sharing of octameric units into 2D layers. AlO_4 tetrahedra with darker shading, PO_4 tetrahedra with lighter shading.

7a). Some gallium phosphates with the same SBU have also been reported.¹⁸ In these cases, the SBU is distorted by fluorine atoms. The ZON and AFR topologies can also be described as covalently bonded layers composed of vertex-sharing building units with different orientations (Fig. 6b and 7b). The ZON topology, as with UiO-28, has a two-dimensional 8-ring channel system, while the two-dimensional channel system in the AFR topology is composed of an 8- and a 12-ring. These three topologies illustrate how a specific secondary building unit can be assembled in three dimensions leading to different frameworks depending on the mode of interconnection between the SBUs. Very recently, a computational approach for predicting crystal structures has been reported.¹⁹ The methodology, denoted automated assembly of secondary building units (AASBU), offers a means of constructing periodic structures of inorganic solids from predefined secondary building units. We expect that this algorithm will be able to construct a number of new topologies based on the SBU now identified in the UiO-28, ZON, AFR and TMP-GaPO topologies.

References

- 1 B. M. Weckhuysen, R. R. Rao, J. A. Martens and R. A. Schoonheydt, *Eur. J. Inorg. Chem.*, 1999, 565.
- 2 J. M. Bennett and B. K. Marcus, in *Innovations in Zeolite Material Science*, eds. P. J. Grobet, W. J. Mortier, E. F. Vansant and G. SchulzEkloff, Elsevier Science Publishers, Amsterdam, 1987, p. 269.

- 3 P. Y. Feng, X. H. Bu and G. D. Stucky, *Nature*, 1997, **388**, 735.
- 4 X. H. Bu, P. Y. Feng and G. D. Stucky, *Science*, 1997, **278**, 2080.
- 5 SAINT Integration Software Version 4.05, Bruker Analytical X-Ray Instruments Inc., Madison, WI, USA, 1995.
- 6 G. M. Sheldrick, SADABS, Empirical Absorption Corrections Program, University of Göttingen, Germany, 1997.
- 7 G. M. Sheldrick, SHELXTL Version 5.0, Bruker Analytical X-Ray Instruments Inc., Madison, WI, USA, 1994.
- 8 P. E. Werner, L. Eriksson and J. Westdahl, *J. Appl. Crystallogr.*, 1985, **18**, 367.
- 9 A. Larson and R. B. von Dreele, GSAS, LANSCE, Generalized Structure Analysis System, University of California, USA, 1985–1988.
- 10 I. D. Brown and D. Altermatt, *Acta Crystallogr., Sect. B*, 1985, **41**, 244.
- 11 X. H. Bu, P. Y. Feng, T. E. Gier and G. D. Stucky, *Microporous Mesoporous Mater.*, 1998, **25**, 109.
- 12 B. Marler, J. Patarin and L. Sierra, *Microporous Mater.*, 1995, **5**, 151.
- 13 D. E. Akporiaye, H. Fjellvåg, E. N. Halvorsen, J. Hustveit, A. Karlsson and K. P. Lillerud, *J. Phys. Chem.*, 1996, **100**, 16641.
- 14 A. Meden, R. W. GrosseKunstleve, C. Baerlocher and L. B. McCusker, *Z. Kristallogr.*, 1997, **212**, 801.
- 15 M. A. Estermann, L. B. McCusker and C. Baerlocher, *J. Appl. Crystallogr.*, 1992, **25**, 539.
- 16 L. B. McCusker and C. Baerlocher, *Microporous Mater.*, 1996, **6**, 51.
- 17 V. Ramaswamy, L. B. McCusker and C. Baerlocher, *Microporous Mesoporous Mater.*, 1999, **31**, 1.
- 18 V. Much, F. Taulelle, T. Loiseau, G. Ferey, A. K. Cheetham, S. Weigel and G. D. Stucky, *Magn. Reson. Chem.*, 1999, **37**, S100.
- 19 C. M. Draznieks, J. M. Newsam, A. M. Gorman, C. M. Freeman and G. Ferey, *Angew. Chem., Int. Ed.*, 2000, **39**, 2270.